

Coordination Chemistry of a Novel Tetramacrocyclic Ligand Derived from 1,4,7-Triazacyclononane: Synthesis, Structure, and Properties of Nickel(II) and Copper(II) Complexes

Bim Graham,[†] Martin J. Grannas,[†] Milton T. W. Hearn,[‡] Christopher M. Kepert,[†] Leone Spiccia,^{*,†} Brian W. Skelton,[§] and Allan H. White[§]

Department of Chemistry, Monash University, Clayton, Victoria 3168, Australia, Centre for Bioprocess Technology, Department of Biochemistry, Monash University, Clayton, Victoria 3168, Australia, and Department of Physical and Inorganic Chemistry, University of Western Australia, Nedlands, Western Australia 6907, Australia

Received September 10, 1999

A new polynucleating ligand, 1,2,4,5-tetrakis(1,4,7-triazacyclonon-1-ylmethyl)benzene (L^{dur}), has been prepared and characterized as its dodecahydrobromide salt. Addition of base to an aqueous solution of this salt and 4 molar equivalents (m.e.) of a Ni(II) salt produces a mixture of bi- and trinuclear complexes, which can be separated by cation-exchange chromatography (CEC) and crystallized as $[Ni_2L^{dur}](ClO_4)_4 \cdot 2H_2O$ (**1**) and $[Ni_3L^{dur}(H_2O)_6](ClO_4)_6 \cdot 9H_2O$ (**2**). The “full capacity” tetranuclear complex, $[Ni_4L^{dur}(H_2O)_{12}](ClO_4)_8 \cdot 8H_2O$ (**3**), is obtained by slow addition of L^{dur} to a refluxing aqueous solution of excess Ni^{2+} ions, followed by CEC purification. Treatment of L^{dur} with 4 m.e. of a copper(II) salt produces exclusively the tetranuclear complex, $[Cu_4L^{dur}(H_2O)_8](ClO_4)_8 \cdot 9H_2O$ (**4**), while reaction with only 2 m.e. of Cu^{2+} ions yields the binuclear complex, $[Cu_2L^{dur}](ClO_4)_4 \cdot 4H_2O$ (**5**). The X-ray structures of complexes **1**, **2**, **4**, and $[Cu_2L^{dur}](ClO_4)_4 \cdot 3H_2O$ (**5'**) have been determined; all are monoclinic, $P2_1/c$: for **1**, $a = 9.497(3)$ Å, $b = 13.665(5)$ Å, $c = 19.355(6)$ Å, $\beta = 100.57(2)^\circ$, $V = 2469(1)$ Å³, and $Z = 2$; for **2**, $a = 22.883(7)$ Å, $b = 15.131(6)$ Å, $c = 20.298(8)$ Å, $\beta = 97.20(3)^\circ$, $V = 6973(4)$ Å³, and $Z = 4$; for **4**, $a = 16.713(7)$ Å, $b = 16.714(6)$ Å, $c = 14.775(11)$ Å, $\beta = 108.24(5)^\circ$, $V = 3920(4)$ Å³, and $Z = 2$; and for **5'**, $a = 9.5705(1)$ Å, $b = 13.0646(1)$ Å, $c = 20.1298(2)$ Å, $\beta = 103.1618(8)^\circ$, $V = 2450.81(4)$ Å³, and $Z = 2$. The metal centers in **1** and **5'** lie in distorted octahedral environments, each facially coordinated by two of the triamine rings of L^{dur} , the cation in each case being centrosymmetric. In **2**, one of the nickel(II) centers is similarly sandwiched by two triamine rings, while the other two nickel(II) centers are each coordinated by a single triamine ring from the ligand, with their distorted octahedral coordination spheres each being completed by three water molecules. In **4**, the four triamine rings of L^{dur} bind to separate copper(II) centers, with two water molecules occupying the remaining two sites of the distorted square pyramidal (SP) coordination spheres, the cation again being centrosymmetric.

Introduction

The covalent linkage of multiple macrocyclic rings has proven to be an effective method for producing ligands capable of holding two or more metal centers in close proximity and in specific spatial arrangements. This has paved the way for the rational design and synthesis of polynuclear complexes, which find application as catalysts,^{1–4} as models for metallobiosites,^{1–10}

and in studies of cation–cation interactions over short interatomic distances.^{6–17}

Our own work has focused on the use of 1,4,7-triazacyclononane (tacn) as a building block in the construction of such systems.^{10,17–19} This facially coordinating tridentate macrocycle has previously been incorporated into bis(macrocycles) containing, for example, alkane,^{5,6,20–23} alcohol,⁷ ether,²¹ xylene,^{13,19} phenol,⁸ pyrazole¹¹ and naphthalene² bridging units. In a few

[†] Department of Chemistry, Monash University.

[‡] Centre for Bioprocess Technology, Department of Biochemistry, Monash University.

[§] University of Western Australia.

(1) Vance, D. H.; Czarnik, A. W. *J. Chem. Soc.* **1993**, 115, 12165.

(2) Young, M. J.; Chin, J. *J. Am. Chem. Soc.* **1995**, 117, 10577.

(3) Chapman, W. H.; Breslow, R. *J. Am. Chem. Soc.* **1995**, 117, 5462.

(4) Fujioka, H.; Koike, T.; Yamada, N.; Kimura, E. *Heterocycles* **1996**, 42, 775.

(5) Wieghardt, K.; Tolksdorf, I.; Herrmann, W. *Inorg. Chem.* **1985**, 24, 1230.

(6) Sessler, J. L.; Sibert, J. W.; Burrell, A. K.; Lynch, V.; Markert, J. T.; Wooten, C. L. *Inorg. Chem.* **1993**, 32, 621.

(7) Sessler, J. L.; Sibert, J. W.; Burrell, A. K.; Lynch, V.; Markert, J. T.; Wooten, C. L. *Inorg. Chem.* **1993**, 32, 4277.

(8) Chang, H.; Diril, H.; Nilges, M. J.; Zhang, X.; Potenza, J. A.; Schugar, H. J.; Hendrickson, D. N.; Isied, S. S. *J. Am. Chem. Soc.* **1988**, 110, 625.

(9) Tolman, W. B. *Acc. Chem. Res.* **1997**, 30, 227.

(10) Spiccia, L.; Graham, B.; Hearn, M. T. W.; Lazarev, G.; Moubaraki, B.; Murray, K. S.; Tiekink, E. R. T. *J. Chem. Soc., Dalton Trans.* **1997**, 4089.

(11) Behle, L.; Neuburger, M.; Zehnder, M.; Kaden, T. A. *Helv. Chim. Acta* **1995**, 78, 693.

(12) Beer, P. D.; Drew, M. G. B.; Leeson, P. B.; Lyssenko, K.; Ogden, M. I. *J. Chem. Soc., Chem. Commun.* **1995**, 929.

(13) Farrugia, L. J.; Lovatt, P. A.; Peacock, R. D. *J. Chem. Soc., Dalton Trans.* **1997**, 911.

(14) Ciampolini, M.; Fabbrizzi, L.; Perotti, A.; Poggi, A.; Seghi, B.; Zanolini, F. *Inorg. Chem.* **1987**, 26, 3527.

(15) Foster, K. A.; Brown, D. R.; Timken, M. D.; Van Derveer, D. G.; Belford, R. L.; Barefield, E. K. *J. Coord. Chem.* **1988**, 19, 123.

(16) Spreer, L. O.; Li, A.; MacQueen, D. B.; Allan, C. B.; Otvos, J. W.; Calvin, M.; Frankel, R. B.; Papaefthymiou, G. C. *Inorg. Chem.* **1994**, 33, 1753.

instances, structurally more elaborate systems have been produced through N-functionalization of bis(tacn) ligands with potentially coordinating pendant arms^{17,18,24} or noncoordinating alkyl groups.^{9,12,25} The popularity of the tacn macrocycle in such ligands stems from its ability to form stable complexes with many metal ions while leaving coordination sites available for the attachment of substrate molecules or for forming polynuclear complexes.

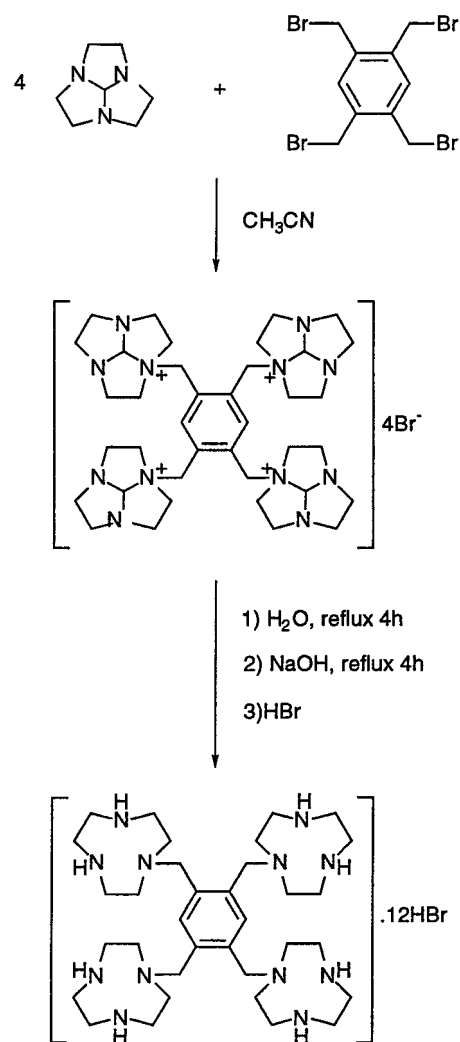
Recently we extended methods for the preparation of bis(tacn) ligands to the synthesis of a trinucleating ligand consisting of three tacn rings linked by a mesitylene bridging unit.¹⁰ The ability of this ligand to act as a template to models for the trinuclear sites of multicopper oxidase enzymes was demonstrated through the self-assembly of a novel polymeric copper(II) complex containing trinuclear sites in which three copper(II) centers are linked by a phosphate bridge. As part of ongoing efforts to produce novel polynuclear metal complexes, we have synthesized a further member of the poly(tacn) series, 1,2,4,5-tetrakis(1,4,7-triazacyclonon-1-ylmethyl)benzene (L^{dur}), incorporating four tacn rings linked by a durene unit (Scheme 1). It was anticipated that L^{dur} would be able to adopt several coordination modes since we have shown that a related *o*-xylylene-bridged bis(tacn) ligand, 1,2-bis(1,4,7-triazacyclonon-1-ylmethyl)benzene (L^{ox}), can form binuclear or mononuclear complexes in which the two tacn rings respectively bind separate metal centers or sandwich a single metal center.¹⁹ These expectations were confirmed through a study of the coordination behavior of L^{dur} toward nickel(II) and copper(II), the results of which are described herein.

Experimental Section

Materials and Reagents. Reagent or analytical grade materials were obtained from commercial suppliers and used without further purification. Acetonitrile and toluene were dried over 4 Å molecular sieves. Distilled water was used throughout. 1,4,7-Triazatricyclo[5.2.1.0^{4,10}]decane²² and 1,2,4,5-tetra(bromomethyl)benzene²⁶ were synthesized according to published methods.

Physical Measurements. Proton and carbon NMR spectra were recorded for D₂O solutions on a Bruker AC200 spectrometer and are referenced to an internal standard of sodium 3-(trimethylsilyl)propionate-2,2,3,4-*d*₄ and an external standard of tetramethylsilane, respectively. Infrared spectra were recorded on a Perkin-Elmer 1600 FTIR spectrophotometer as KBr pellets or Nujol mulls and electronic spectra on a Cary 5G UV-vis-near-IR spectrophotometer. Electron microprobe analyses were made with a JEOL JSM-1 scanning electron microscope through an NEC X-ray detector and pulse-processing system connected to a Packard multichannel analyzer. A Micromass Platform

Scheme 1. Preparation of $L^{\text{dur}} \cdot 12\text{HBr}$



quadrupole mass spectrometer was used to record electrospray ionization (ESI) mass spectra on 50% $\text{CH}_3\text{CN}/\text{H}_2\text{O}$ solutions. Quoted m/z values refer to the most intense peak in each signal envelope. Room-temperature magnetic moments were determined by the Faraday method. ESR spectra were recorded on a Varian E-12 spectrometer as frozen (77 K) DMF solutions and simulated with the aid of the Bruker Simfonia program.

CAUTION! Although no problems were encountered in this work, perchlorate salts of transition metal complexes are potentially explosive and should therefore be prepared in small quantities and handled with due care.

Preparations. 1,2,4,5-Tetrakis(1,4,7-triazacyclonon-1-ylmethyl)benzene Dodecahydrobromide Nonahydrate ($L^{\text{dur}} \cdot 12\text{HBr} \cdot 9\text{H}_2\text{O}$). A solution of 1,2,4,5-tetra(bromomethyl)benzene (1.60 g, 3.56 mmol) in CH_3CN (30 mL) was added dropwise to a stirred solution of 1,4,7-triazatricyclo[5.2.1.0^{4,10}]decane (2.00 g, 14.4 mmol) in CH_3CN (30 mL) over a period of 2 h, resulting in the formation of a white precipitate. After stirring overnight, the precipitate was filtered off, washed with CH_3CN (10 mL), and dried in a vacuum desiccator. The solid was then dissolved in H_2O (50 mL) and refluxed for 4 h. NaOH pellets (4.00 g, 100 mmol) were carefully added in portions to the solution, and refluxing was continued for a further 4 h. Most of the solvent was removed on a rotary evaporator, then toluene (100 mL) was added, and the residual H_2O was distilled off using a Dean-Stark azeotropic apparatus. The toluene solution was filtered while hot to remove the precipitate of NaBr and NaOH which formed. The solid residue was then extracted twice with hot toluene (50 mL), and the combined toluene fractions were reduced to dryness on a rotary evaporator to yield a light yellow oil. This was dissolved in 3 mL of H_2O and 50 mL of

- (17) (a) Brudenell, S. J.; Spiccia, L.; Tiekink, E. R. T. *Inorg. Chem.* **1996**, 35, 1974. (b) Brudenell, S. J.; Spiccia, L.; Bond, A. M.; Comba, P.; Hockless, D. C. R. *Inorg. Chem.* **1996**, 35, 1974. (c) Brudenell, S. J.; Spiccia, L.; Bond, A. M.; Mahon, P. C.; Hockless, D. C. R. *J. Chem. Soc., Dalton Trans.* **1998**, 3919. (d) Brudenell, S. J.; Spiccia, L.; Hockless, D. C. R.; Tiekink, E. R. T. *J. Chem. Soc., Dalton Trans.* **1999**, 1475.
- (18) Fry, F. H.; Graham, B.; Spiccia, L.; Hockless, D. C. R.; Tiekink, E. R. T. *J. Chem. Soc., Dalton Trans.* **1997**, 827.
- (19) Graham, B.; Fallon, G. D.; Hearn, M. T. W.; Hockless, D. C. R.; Lazarev, G.; Spiccia, L. *Inorg. Chem.* **1997**, 36, 6366.
- (20) Tanaka, N.; Kobayashi, Y.; Takamoto, S. *Chem. Lett.* **1977**, 107.
- (21) Weisman, G. R.; Vachon, D. J.; Johnson, V. B.; Gronbeck, D. A. *J. Chem. Soc., Chem. Commun.* **1987**, 886.
- (22) Zhang, X.; Hsieh, W.-Y.; Margulis, T. N.; Zompa, L. *J. Inorg. Chem.* **1995**, 34, 2883.
- (23) Haidar, R.; Ipek, M.; DasGupta, B.; Yousaf, M.; Zompa, L. *Inorg. Chem.* **1997**, 36, 3125.
- (24) Blake, A. J.; Donlevy, T. M.; England, P. A.; Fallis, I. A.; Parsons, S.; Schröder, M. *J. Chem. Soc., Chem. Commun.* **1994**, 1981.
- (25) Hanke, D.; Wiegardt, K.; Nuber, B.; Lu, R.-S.; McMullan, R. K.; Koetzie, T. F.; Bau, R. *Inorg. Chem.* **1993**, 32, 4300.
- (26) Ried, W.; Bodem, H. *Chem. Ber.* **1956**, 89, 2328.

48% HBr added dropwise. Addition of 50 mL of absolute EtOH (50 mL) afforded a white product, which was collected by vacuum filtration, washed with EtOH and Et₂O, and dried in a vacuum desiccator. Yield: 3.59 g, 59%. Anal. Calcd for C₃₄H₉₆Br₁₂N₁₂O₉ (L·12HBr·9H₂O): C, 23.0; H, 5.3; N, 9.5. Found: C, 22.7; H, 5.4; N, 9.8. ¹H NMR: δ 3.06 (16H, t, tacn ring CH₂), 3.24 (16H, t, tacn ring CH₂), 3.71 (16H, s, tacn ring CH₂), 4.17 (8H, s, bridge CH₂), 7.79 (2H, s, aromatic CH). ¹³C NMR: δ 42.31, 44.09, 48.12 (tacn ring CH₂), 55.06 (bridge CH₂), 134.35 (aromatic CH), 135.28 (aromatic quaternary C).

[Ni₂L^{dur}(ClO₄)₄·2H₂O (1) and [Ni₃L^{dur}(H₂O)₆](ClO₄)₆·9H₂O (2). To an aqueous solution (50 mL) of L^{dur}·12HBr·9H₂O (1.80 g, 1.01 mmol) and Ni(NO₃)₂·6H₂O (1.18 g, 4.06 mmol), heated on a steam bath, was added 2 M NaOH dropwise until a small amount of nickel hydroxide precipitate appeared which would not dissolve on prolonged heating. Sufficient 2 M HCl was then added to just dissolve this precipitate and the resulting purple-blue solution heated for an additional 15 min before being diluted to 2 L with H₂O and loaded onto a Sephadex SP-C25 cation-exchange column (H⁺ form, 15 × 4 cm). After washing with H₂O and 0.3 M NaClO₄ (to remove excess Ni²⁺), a pink band was eluted from the column with 0.5 M NaClO₄. This fraction yielded pink crystals of **1** on standing overnight, which were collected by vacuum filtration, washed with MeOH, and air-dried. Yield: 0.26 g, 22%. Anal. Calcd for C₃₄H₇₀Cl₄N₁₂Ni₂O₁₈ ([Ni₂L^{dur}(ClO₄)₄·2H₂O): C, 34.2; H, 5.9; N, 14.1. Found: C, 34.2; H, 5.5; N, 14.3. Electron microprobe: Ni and Cl present. Selected IR bands (KBr, cm⁻¹): 3420s, 3331s, 3219s, 2938m, 2875m, 1619m, 1479m, 1087s, 952m, 626s. Magnetic moment: μ_{eff} (299 K) = 3.10 μ_B per nickel(II). ESI mass spectrum (*m/z*): 1057.30 {[Ni₂L^{dur}(ClO₄)₃]⁺}, 479.16 {[Ni₂L^{dur}(ClO₄)₂]²⁺}, 286.46 {[Ni₂L^{dur}(ClO₄)₃]³⁺}, 189.61 [Ni₂L^{dur}]⁴⁺. UV-vis-near-IR spectrum in CH₃CN (λ_{max}, nm (ε_{max}, M⁻¹ cm⁻¹): 350 (sh), 539 (12), 620 (sh), 829 (sh), 912 (29)). Crystals of **1** suitable for the X-ray study were grown by diffusion of MeOH into a DMF solution of the complex.

A second purple-pink band was eluted from the Sephadex column using 1.0 M NaClO₄. Slow evaporation of this fraction over 2 days yielded light purple crystals of **2** suitable for crystallographic study. These were collected by vacuum filtration, washed quickly with a small amount of cold MeOH, and air-dried. Yield: 0.55 g, 32%. Anal. Calcd for C₃₄H₉₆Cl₆N₁₂Ni₃O₃₉ ([Ni₃L^{dur}(H₂O)₆](ClO₄)₆·9H₂O): C, 24.2; H, 5.7; N, 10.0. Found: C, 24.2; H, 5.7; N, 10.1. Electron microprobe: Ni and Cl present. Selected IR bands (KBr, cm⁻¹): 3487s, 3320s, 2946m, 2885m, 1635s, 1494s, 1459s, 1098s, 949s, 625s. Magnetic moment: μ_{eff} (299 K) = 3.19 μ_B per nickel(II). ESI mass spectrum (*m/z*): 1315.17 {[Ni₃L^{dur}(ClO₄)₅]⁺}, 608.08 {[Ni₃L^{dur}(ClO₄)₄]²⁺}, 372.40 {[Ni₃L^{dur}(ClO₄)₃]³⁺}. UV-vis-near-IR spectrum in water (λ_{max}, nm (ε_{max}, M⁻¹ cm⁻¹): 353 (22), 561 (15), 780 (sh), 942 (51)).

[Ni₄L^{dur}(H₂O)₁₂](ClO₄)₈·8H₂O (3). A solution of L^{dur}·12HBr·9H₂O (0.55 g, 0.31 mmol) in H₂O (50 mL) was adjusted to pH 6–7 with 6 M NaOH and then added dropwise to a refluxing solution of NiCl₂·6H₂O (3.68 g, 15.5 mmol) in H₂O (5 mL) over a period of 2 h. Refluxing was continued for a further 30 min before the solution was diluted to 2 L with H₂O and loaded onto a Sephadex SP-C25 cation-exchange column (H⁺ form, 15 × 4 cm). After washing with H₂O and 0.3 M NaClO₄ (to remove excess Ni²⁺), a purple-pink band of **2** was eluted with 1.0 M NaClO₄, leaving a less mobile purple band of roughly equal intensity, which was eluted using 2.0 M NaClO₄. Slow evaporation over 2 weeks eventually gave some light purple crystals of **3**, which were collected by filtration and washed quickly with a small amount of cold MeOH, a process resulting in loss of product. Yield: 0.09 g, 14%. Anal. Calcd for C₃₄H₁₀₆Cl₈N₁₂Ni₄O₅₂ ([Ni₄L^{dur}(H₂O)₁₂](ClO₄)₈·8H₂O): C, 20.1; H, 5.3; N, 8.3. Found: C, 20.2; H, 5.6; N, 8.0. Electron microprobe: Ni and Cl present. Selected IR bands (KBr, cm⁻¹): 3424s, 3319s, 2932m, 2881m, 1637s, 1492m, 1459m, 1366m, 1090s, 948m, 628s. Magnetic moment: μ_{eff} (299 K) = 3.05 μ_B per nickel(II). ESI mass spectrum (*m/z*): 1572.94 {[Ni₄L^{dur}(ClO₄)₇]⁺}, 736.99 {[Ni₄L^{dur}(ClO₄)₆]²⁺}, 457.68 {[Ni₄L^{dur}(ClO₄)₅]³⁺}. UV-vis-near-IR spectrum in water (λ_{max}, nm (ε_{max}, M⁻¹ cm⁻¹): 350 (sh), 575 (20), 785 (sh), 970 (63)).

[Cu₄L^{dur}(H₂O)₈](ClO₄)₈·9H₂O (4). To a solution of L^{dur}·12HBr·9H₂O (1.00 g, 0.563 mmol) and Cu(NO₃)₂·3H₂O (0.70 g, 2.90 mmol) dissolved in H₂O (50 mL) was added 2 M NaOH until a precipitate of

copper hydroxide began to appear. After sufficient 2 M HCl was added to just dissolve this precipitate, the dark blue solution was diluted to 2 L with H₂O and loaded onto a Sephadex SP-C25 cation-exchange column (H⁺ form, 15 × 4 cm). After washing with H₂O and 0.3 M NaClO₄ (to remove a light green band of excess Cu²⁺), a dark blue band was eluted with 2.0 M NaClO₄ and left to slowly evaporate. Blue crystals suitable for crystallographic study formed over the next 5 days and were collected by vacuum filtration. Yield: 0.39 g, 35%. Prior to analysis the solid was washed quickly with a small amount of cold MeOH, a procedure resulting in loss of product. Anal. Calcd for C₃₄H₁₀₀Cl₈Cu₄N₁₂O₄₉ ([Cu₄L^{dur}(H₂O)₈](ClO₄)₈·9H₂O): C, 20.4; H, 5.0; N, 8.4. Found: C, 20.8; H, 5.0; N, 8.4. Electron microprobe: Cu and Cl present. Selected IR bands (Nujol, cm⁻¹): 3508s, 3304s, 2955s, 1622s, 1491m, 1286m, 1086s, 950m, 624m. Magnetic moment: μ_{eff} (299 K) = 1.90 μ_B per copper(II). ESI mass spectrum (*m/z*): 1592.99 {[Cu₄L^{dur}(ClO₄)₇]⁺}, 746.99 {[Cu₄L^{dur}(ClO₄)₆]²⁺}. Fitted X-band ESR parameters (DMF, 77 K): *g_{xx}* = 2.027, *g_{yy}* = 2.085, *g_{zz}* = 2.284, *A_{xx}* = 0, *A_{yy}* = 0, *A_{zz}* = 170 × 10⁻⁴ cm⁻¹. UV-vis-near-IR spectrum in water (λ_{max}, nm (ε_{max}, M⁻¹ cm⁻¹): 650 (160), 1062 (67)).

[Cu₂L^{dur}(ClO₄)₄·4H₂O (5) and [Cu₂L^{dur}(ClO₄)₄·3H₂O (5'). The pH of an aqueous solution (50 mL) of L^{dur}·12HBr·9H₂O (0.75 g, 0.42 mmol) and Cu(NO₃)₂·3H₂O (0.20 g, 0.83 mmol) was adjusted to ~5 with 2 M NaOH. Excess NaClO₄ (1.00 g) was added to the dark blue solution and the mixture heated on a steam bath for 20 min. Slow evaporation over 3 days gave blue crystals, which were filtered off, washed with a small amount of MeOH, and air-dried. Yield: 0.24 g, 46%. Anal. Calcd for C₃₄H₇₄Cl₄Cu₂N₁₂O₂₀ ([Cu₂L^{dur}(ClO₄)₄·4H₂O): C, 32.9; H, 5.9; N, 13.6. Found: C, 32.9; H, 5.7; N, 13.4. Electron microprobe: Cu and Cl present. Selected IR bands (KBr, cm⁻¹): 3423s, 3226s, 2930m, 1638m, 1491m, 1463m, 1084s, 964m, 626s. Magnetic moment: μ_{eff} (299 K) = 1.92 μ_B per copper(II). ESI mass spectrum (*m/z*): 1067.30 {[Cu₂L^{dur}(ClO₄)₃]⁺}, 484.16 {[Cu₂L^{dur}(ClO₄)₂]²⁺}. Fitted X-band ESR parameters (DMF, 77K): *g_{xx}* = 2.052, *g_{yy}* = 2.052, *g_{zz}* = 2.246, *A_{xx}* = 0, *A_{yy}* = 25 × 10⁻⁴ cm⁻¹, *A_{zz}* = 170 × 10⁻⁴ cm⁻¹. UV-vis-near-IR spectrum in water (λ_{max}, nm (ε_{max}, M⁻¹ cm⁻¹): 652 (191), 1062 (63)). Slow evaporation of a CH₃CN solution of **5** containing an excess of Bu₄NClO₄ gave crystals of **5'** suitable for X-ray study.

Crystallography. Unique four-circle diffractometer data sets (2θ/θ scan mode) were measured for **1**, **2**, and **4** on an Enraf-Nonius CAD-4 diffractometer, while two sets of data (180° in φ, 106° in ω) were measured for **5'** on an Enraf-Nonius Kappa CCD diffractometer, yielding *N* independent reflections. For each set of data, reflections with *I* > 3σ(*I*) were considered "observed" and used in the full matrix/large block least squares refinement (after Gaussian absorption correction in the case of **1**, **2**, and **4**). Anisotropic thermal parameters were refined for the non-hydrogen atoms, (*x*, *y*, *z*, *U*_{iso})_H being included constrained at estimated values. Substantial difference map residues were modeled as the oxygen atoms of water molecules of solvation. Conventional residuals *R*, *R_w* on |*F*| at convergence are cited, statistical weights derivative of σ²(*I*) = σ²(*I*_{diff}) + 0.0004σ⁴(*I*_{diff}) being used for **1**, **2**, and **4**, and 1/σ²(*F*) for **5'**. Neutral atom complex scattering factors were employed in each case, and computation was carried out using the Xtal 3.4 program system²⁷ for **1**, **2**, and **4**, and texSan²⁸ for **5'**.

The following are specific comments about the solution of the structure of each complex: (i) Water molecule hydrogen atoms were not located for **1**. (ii) In the case of **2**, weak and limited data would support meaningful anisotropic thermal parameter refinement for Ni, Cl, and perchlorate oxygen atoms only, except those associated with Cl(5). (iii) In the case of **4**, a hemisphere of data was measured, *R*_{int} after absorption correction being 0.035. As in the above determinations, perchlorate thermal motion/disorder presented serious problems in modeling. In the present case, the oxygen atoms of perchlorate **4** were disordered over two sets of sites, occupancies set at 0.5 after trial refinement with isotropic thermal parameter forms, and geometries (together with those of perchlorate **1**) constrained to estimated values. For solvent O(5), site occupancy was set at 0.5 after trial refinement.

(27) Hall, S. R.; King, G. S. D.; Stewart, J. M. *The Xtal 3.4 User's Manual*; University of Western Australia, Lamb Print: Perth, 1994.

(28) *teXsan: Crystal Structure Analysis Package*; Molecular Structure Corporation: Houston, TX, 1985 and 1992.

Table 1. Crystallographic Data for $[\text{Ni}_2\text{L}^{\text{dur}}](\text{ClO}_4)_4 \cdot 2\text{H}_2\text{O}$ (**1**), $[\text{Ni}_3\text{L}^{\text{dur}}(\text{H}_2\text{O})_6](\text{ClO}_4)_6 \cdot \text{ca.}9\text{H}_2\text{O}$ (**2**), $[\text{Cu}_4\text{L}^{\text{dur}}(\text{H}_2\text{O})_8](\text{ClO}_4)_8 \cdot \text{ca.}9\text{H}_2\text{O}$ (**4**), and $[\text{Cu}_2\text{L}^{\text{dur}}](\text{ClO}_4)_4 \cdot 3\text{H}_2\text{O}$ (**5'**)

	1	2	4	5'
formula	$\text{C}_{34}\text{H}_{70}\text{Cl}_4\text{N}_{12}\text{Ni}_2\text{O}_{18}$	$\text{C}_{34}\text{H}_{96}\text{Cl}_6\text{N}_{12}\text{Ni}_3\text{O}_{39}$	$\text{C}_{34}\text{H}_{100}\text{Cl}_8\text{Cu}_4\text{N}_{12}\text{O}_{49}$	$\text{C}_{34}\text{H}_{72}\text{Cl}_4\text{Cu}_2\text{N}_{12}\text{O}_{19}$
fw	1194.21	1686.07	1999.04	1221.93
cryst syst	monoclinic	monoclinic	monoclinic	monoclinic
cryst size, mm	$0.30 \times 0.10 \times 0.40$	$0.20 \times 0.35 \times 0.15$	$0.20 \times 0.55 \times 0.72$	$0.13 \times 0.18 \times 0.38$
space group	$P2_1/c$ (C_{2h}^5 , No. 14)	$P2_1/c$ (C_{2h}^5 , No. 14)	$P2_1/c$ (C_{2h}^5 , No. 14)	$P2_1/c$ (C_{2h}^5 , No. 14)
<i>a</i> , Å	9.497(3)	22.883(7)	16.713(7)	9.5705(1)
<i>b</i> , Å	13.665(5)	15.131(6)	16.714(6)	13.0646(1)
<i>c</i> , Å	19.355(6)	20.298(8)	14.775(14)	20.1298(2)
β , deg	100.57(2)	97.20(3)	108.24(5)	103.1618(8)
<i>V</i> , Å ³	2469(1)	6973(4)	3920(4)	2450.81(4)
<i>Z</i>	2	4	2	2
ρ_{calcd} , g cm ⁻³	1.606	1.606	1.693	1.655
<i>T</i> , °C	20	20	20	-150
radiation (λ , Å)	Mo K α (0.7107)	Mo K α (0.7107)	Mo K α (0.7107)	Mo K α (0.7107)
<i>A</i> _{min,max} *	1.15, 1.20	1.21, 1.45	1.32, 2.16	-
$2\theta_{\text{max}}$, °	50	46	50	55
<i>F</i> (000)	1252	3528	2064	1276
μ , cm ⁻¹	10.6	11.3	14.5	11.70
no. of data measd	4516	10960	13768	28309
<i>N</i>	4188	9671	6898	7302
<i>N</i> _o	2499	2024	3259	5618
<i>R</i> ^a	0.063	0.115	0.084	0.042
<i>R</i> _w ^b	0.070	0.098	0.099	0.054

$$^a R = \frac{\sum(\Delta|F|)}{\sum|F_o|}, \quad ^b R_w = \frac{[\sum w(\Delta|F|)^2/\sum wF_o^2]^{1/2}}{[\sigma^2(F_o)]^{-1}}$$

(iv) In the case of **5'**, residual electron peaks due to disorder in perchlorate counterions could not be reasonably modeled and hence resulting in higher residuals with high anisotropic thermal parameters for the perchlorate oxygens closest to the largest peaks, possibly a foil for unresolved disorder.

Crystal parameters and details of the data collection and refinement for **1**, **2**, **4** and **5'** are summarized in Table 1. Selected bond lengths and angles are given in Table 2 and views of the cation units of the complexes in Figures 1–4, 20% thermal envelopes being shown for the room-temperature determinations and 30% for the low temperature study (Figure 2).

Results and Discussion

Preparation of Ligand. The synthesis of the new tetrakis-(1,4,7-triazacyclonon-1-yl) ligand, L^{dur} , was adapted from the methods described recently for the related xylylene-bridged bis-(macrocycles)^{13,19} and a mesitylene-bridged tris(macrocycle).¹⁰ This involved reaction of the orthoamide derivative of tacn (1,4,7-triazatricyclo[5.2.1.0^{4,10}]decane) with 1,2,4,5-tetra(bromomethyl)benzene (in a 4:1 molar ratio), followed by base hydrolytic workup to yield the target compound in good yield (Scheme 1). The ligand was isolated as its nonhygroscopic dodecahydrobromide salt. The relatively simple ¹³C NMR of L^{dur} confirms the symmetric nature of the ligand. Three clearly resolved signals are observed at 42.31, 44.09, and 48.12 ppm, corresponding to the three unique methylene carbons of the tacn rings. The four equivalent methylene carbons of the durene bridging unit are deshielded as a result of the aromatic ring current and consequently appear further downfield at 55.06 ppm. Signals corresponding to the aromatic CH and quaternary carbons are observed at 134.35 and 135.28 ppm, respectively.

Preparation of Metal Complexes. It was anticipated that treatment of L^{dur} with 4 m.e. of a transition metal salt would yield tetranuclear complexes in which each tacn macrocycle facially coordinated to a different metal center. For nickel(II), however, simple treatment of an aqueous solution of $\text{Ni}(\text{NO}_3)_2 \cdot 6\text{H}_2\text{O}$ and $\text{L}^{\text{dur}} \cdot 12\text{HBr} \cdot 9\text{H}_2\text{O}$ in a 4:1 molar ratio with base produces a mixture of bi- and trinuclear species. These are readily separable by CEC and, once separated, showed no evidence of rearrangement in solution. The products were crystallized as $[\text{Ni}_2\text{L}^{\text{dur}}](\text{ClO}_4)_4 \cdot 2\text{H}_2\text{O}$ (**1**) and $[\text{Ni}_3\text{L}^{\text{dur}}(\text{H}_2\text{O})_6]$ -

$(\text{ClO}_4)_6 \cdot 9\text{H}_2\text{O}$ (**2**), respectively, on slow evaporation at ambient temperatures. Production of sufficient quantities of the tetranuclear species for crystallization of its perchlorate salt, $[\text{Ni}_4\text{L}^{\text{dur}}(\text{H}_2\text{O})_{12}](\text{ClO}_4)_8 \cdot 8\text{H}_2\text{O}$ (**3**), was eventually achieved by an alternative route involving slow addition of a neutral aqueous solution of L^{dur} to a refluxing aqueous solution containing 50 molar equiv of Ni^{2+} . This yielded a mixture containing approximately equal amounts of **2** and **3** which, once again, could be separated by CEC.

The formation of bi-, tri-, and tetranuclear complexes of the L^{dur} ligand highlights the ability of the two pairs of *ortho*-oriented tacn rings in the ligand to either sandwich a single nickel(II) center or coordinate to two separate nickel(II) centers (Figure 5). The variable coordination modes of L^{dur} are reminiscent of those of the *o*-xylylene-bridged bis(tacn) ligand, L^{ox} , which can act as a bis(tridentate) ligand, coordinating to two nickel(II) centers, or as a hexadentate ligand, sandwiching a single nickel(II) center between the two tacn rings.¹⁹

In contrast to its coordination behavior toward nickel(II), reaction of L^{dur} with 4 m.e. of a copper(II) salt gave exclusively the tetranuclear complex, $[\text{Cu}_4\text{L}^{\text{dur}}(\text{H}_2\text{O})_8](\text{ClO}_4)_8 \cdot 9\text{H}_2\text{O}$ (**4**). The binuclear complex, $[\text{Cu}_2\text{L}^{\text{dur}}](\text{ClO}_4)_4 \cdot 4\text{H}_2\text{O}$ (**5**), was formed by adding 2 m.e. of $\text{Cu}(\text{NO}_3)_2 \cdot 3\text{H}_2\text{O}$ to an aqueous solution of $\text{L}^{\text{dur}} \cdot 12\text{HBr} \cdot 9\text{H}_2\text{O}$ at pH 5 and addition of excess NaClO_4 . Recrystallization of **5** from acetonitrile yielded $[\text{Cu}_2\text{L}^{\text{dur}}](\text{ClO}_4)_4 \cdot 3\text{H}_2\text{O}$ (**5'**). These results are in accord with our previous findings for the bis(macrocycle), L^{ox} , which forms a binuclear complex with one copper(II) center coordinated to each tacn ring when excess metal ion is used and the mononuclear sandwich complex when a 1:1 M:L ratio is used.¹⁹ Compounds **4** and **5'** have structures analogous to the “full capacity” and “double sandwich” structures of **3** and **1**, respectively, except that the copper(II) centers in **4** are five-coordinate, with only two water molecules coordinating to each metal ion (see crystal structures).

Analytical data for each of the nickel(II) and copper(II) complexes of L^{dur} are consistent with the given compositions. In addition, the ESI mass spectra of the complexes, measured in a 1:1 $\text{CH}_3\text{CN}/\text{H}_2\text{O}$ solution, exhibited peak envelopes with isotope distribution patterns consistent with the formulations $\{[\text{Ni}_2\text{L}^{\text{dur}}](\text{ClO}_4)_n\}^{(4-n)+}$ ($n = 0-3$) for **1**, $\{[\text{Ni}_3\text{L}^{\text{dur}}](\text{ClO}_4)_n\}^{(6-n)+}$

Table 2. Metal Atom Environments (Distances (Å) and Angles (deg)) for [Ni₂L^{dur}](ClO₄)₄·2H₂O (**1**), [Ni₃L^{dur}(H₂O)₆](ClO₄)₆·ca.9H₂O (**2**), [Cu₄L^{dur}(H₂O)₈](ClO₄)₈·9H₂O (**4**), and [Cu₂L^{dur}](ClO₄)₄·3H₂O (**5'**)

1		5'		4		2	
Ni–N(11)	2.193(6)	Cu–N(1)	2.089(2)	Cu(1)–O(101)	2.002(7)	Ni(1)–O(301)	2.12(4)
Ni–N(14)	2.149(7)	Cu–N(2)	2.031(2)	Cu(1)–O(102)	1.966(8)	Ni(1)–O(302)	2.02(3)
Ni–N(17)	2.094(6)	Cu–N(3)	2.427(2)	Cu(1)–N(11)	2.29(1)	Ni(1)–O(303)	2.17(3)
Ni–N(21)	2.151(6)	Cu–N(4)	2.506(2)	Cu(1)–N(14)	1.998(8)	Ni(1)–N(11)	2.15(3)
Ni–N(24)	2.134(7)	Cu–N(5)	2.113(2)	Cu(1)–N(17)	1.99(1)	Ni(1)–N(14)	1.98(3)
Ni–N(27)	2.086(7)	Cu–N(6)	2.034(2)	Cu(2)–O(201)	1.98(2)	Ni(1)–N(17)	2.10(4)
				Cu(2)–O(202)	2.02(1)	Ni(2)–O(201)	2.17(3)
				Cu(2)–N(21)	2.251(9)	Ni(2)–O(202)	2.09(3)
				Cu(2)–N(24)	2.04(2)	Ni(2)–O(203)	2.17(3)
				Cu(2)–N(27)	1.99(2)	Ni(2)–N(21)	2.10(2)
						Ni(2)–N(24)	2.02(3)
						Ni(2)–N(27)	1.99(3)
						Ni(3)–N(41)	2.24(3)
						Ni(3)–N(44)	2.14(3)
						Ni(3)–N(47)	2.08(3)
						Ni(3)–N(51)	2.16(3)
						Ni(3)–N(54)	2.13(3)
						Ni(3)–N(57)	2.17(3)
N(11)–Ni–N(14)	80.6(2)	N(1)–Cu–N(2)	84.29(8)	O(101)–Cu(1)–O(102)	88.1(4)	O(301)–Ni(1)–O(302)	85(1)
N(11)–Ni–N(17)	80.0(2)	N(1)–Cu–N(3)	76.94(7)	O(101)–Cu(1)–N(11)	100.4(7)	O(301)–Ni(1)–O(303)	89(1)
N(11)–Ni–N(21)	103.1(2)	N(1)–Cu–N(4)	100.05(7)	O(101)–Cu(1)–N(14)	174.5(4)	O(301)–Ni(1)–N(11)	175(1)
N(11)–Ni–N(24)	106.6(3)	N(1)–Cu–N(5)	104.59(7)	O(101)–Cu(1)–N(17)	92.3(4)	O(301)–Ni(1)–N(14)	92(1)
N(11)–Ni–N(27)	170.8(3)	N(1)–Cu–N(6)	171.85(8)	O(102)–Cu(1)–N(11)	105.3(4)	O(301)–Ni(1)–N(17)	93(1)
N(14)–Ni–N(17)	82.4(3)	N(2)–Cu–N(3)	80.22(8)	O(102)–Cu(1)–N(14)	92.3(4)	O(302)–Ni(1)–O(303)	85(1)
N(14)–Ni–N(21)	103.9(2)	N(2)–Cu–N(4)	125.24(8)	O(102)–Cu(1)–N(17)	171.9(5)	O(302)–Ni(1)–N(11)	100(1)
N(14)–Ni–N(24)	169.2(2)	N(2)–Cu–N(5)	157.28(8)	N(11)–Cu(1)–N(14)	84.7(4)	O(302)–Ni(1)–N(14)	100(1)
N(14)–Ni–N(27)	90.3(3)	N(2)–Cu–N(6)	89.81(8)	N(11)–Cu(1)–N(17)	82.6(4)	O(302)–Ni(1)–N(17)	177(1)
N(17)–Ni–N(21)	173.4(3)	N(3)–Cu–N(4)	154.28(7)	N(14)–Cu(1)–N(17)	86.5(4)	O(303)–Ni(1)–N(11)	94(1)
N(17)–Ni–N(24)	90.9(3)	N(3)–Cu–N(5)	81.51(7)	O(201)–Cu(2)–O(202)	86.8(7)	O(303)–Ni(1)–N(14)	176(1)
N(17)–Ni–N(27)	97.7(3)	N(3)–Cu–N(6)	107.65(8)	O(201)–Cu(2)–N(21)	102.1(5)	O(303)–Ni(1)–N(17)	93(1)
N(21)–Ni–N(24)	82.6(2)	N(4)–Cu–N(5)	74.49(7)	O(201)–Cu(2)–N(24)	173.7(5)	N(11)–Ni(1)–N(14)	85(1)
N(21)–Ni–N(27)	80.2(2)	N(4)–Cu–N(6)	78.77(7)	O(201)–Cu(2)–N(27)	90.9(7)	N(11)–Ni(1)–N(17)	82(1)
N(24)–Ni–N(27)	82.3(3)	N(5)–Cu–N(6)	82.96(8)	O(202)–Cu(2)–N(21)	101.4(4)	N(14)–Ni(1)–N(17)	83(1)
				O(202)–Cu(2)–N(24)	96.0(7)	O(201)–Ni(2)–O(202)	87(1)
				O(202)–Cu(2)–N(27)	174.2(6)	O(201)–Ni(2)–O(203)	83(1)
				N(21)–Cu(2)–N(24)	82.9(5)	O(201)–Ni(2)–N(21)	95(1)
				N(21)–Cu(2)–N(27)	84.3(5)	O(201)–Ni(2)–N(24)	94(1)
				N(24)–Cu(2)–N(27)	85.8(8)	O(201)–Ni(2)–N(27)	178(1)
						O(202)–Ni(2)–O(203)	87(1)
						O(202)–Ni(2)–N(21)	96(1)
						O(202)–Ni(2)–N(24)	178(1)
						O(202)–Ni(2)–N(27)	91(1)
						O(203)–Ni(2)–N(21)	176(1)
						O(203)–Ni(2)–N(24)	91(1)
						O(203)–Ni(2)–N(27)	96(1)
						N(21)–Ni(2)–N(24)	88(1)
						N(21)–Ni(2)–N(27)	86(1)
						N(24)–Ni(2)–N(27)	86(1)
						N(41)–Ni(3)–N(44)	81(1)
						N(41)–Ni(3)–N(47)	81(1)
						N(41)–Ni(3)–N(51)	102(1)
						N(41)–Ni(3)–N(54)	107(1)
						N(41)–Ni(3)–N(57)	170(1)
						N(44)–Ni(3)–N(47)	82(1)
						N(44)–Ni(3)–N(51)	174(1)
						N(44)–Ni(3)–N(54)	92(1)
						N(44)–Ni(3)–N(57)	101(1)
						N(47)–Ni(3)–N(51)	103(1)
						N(47)–Ni(3)–N(54)	169(1)
						N(47)–Ni(3)–N(57)	89(1)
						N(51)–Ni(3)–N(54)	82(1)
						N(51)–Ni(3)–N(57)	79(1)
						N(54)–Ni(3)–N(57)	83(1)

($n = 3-5$) for **2**, {[Ni₄L^{dur}](ClO₄)_n}⁽⁸⁻ⁿ⁾⁺ ($n = 5-7$) for **3**, {[Cu₄L^{dur}](ClO₄)_n}⁽⁸⁻ⁿ⁾⁺ ($n = 6, 7$) for **4**, and {[Cu₂L^{dur}](ClO₄)_n}⁽⁴⁻ⁿ⁾⁺ ($n = 2, 3$) for **5**. Water ligands were lost from the metal coordination spheres of **2-4** under the experimental conditions. Magnetic and electronic spectral data for **1-3** are typical of octahedral nickel(II) complexes while **4** and **5** exhibit

electronic and ESR spectra typical of SP or tetragonally distorted octahedral copper(II) centers.

Crystal Structures. The crystal structures of **1** and **5'** consist of discrete dinuclear [M₂L^{dur}]⁴⁺ cations (**1**, M = Ni, Figure 1; **5'**, M = Cu, Figure 2), perchlorate anions, and waters of crystallization. In both cations, the two metal centers are each

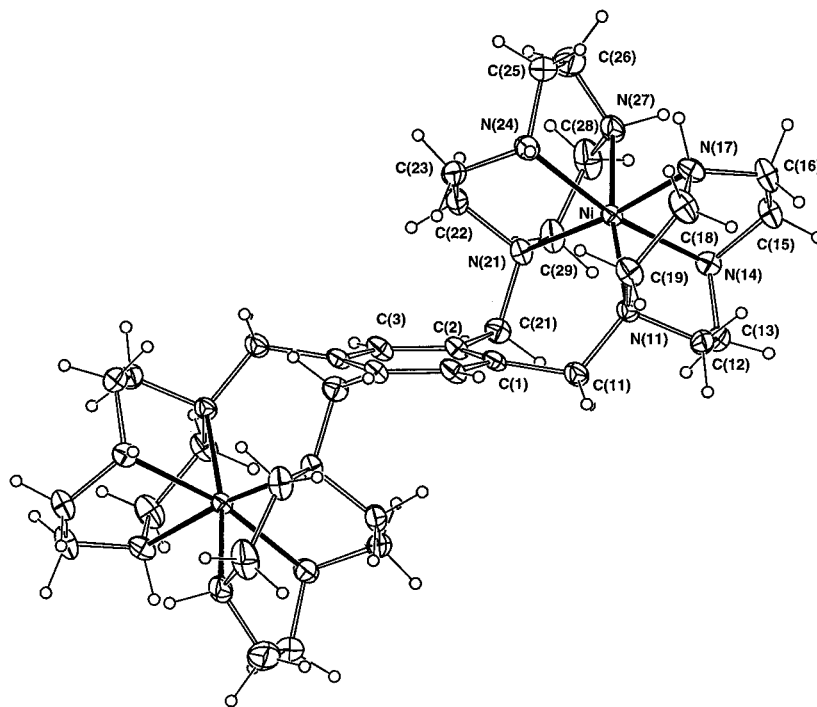


Figure 1. The centrosymmetric binuclear cation unit of **1**, projected through the central benzene ring plane, with the atomic labeling scheme.

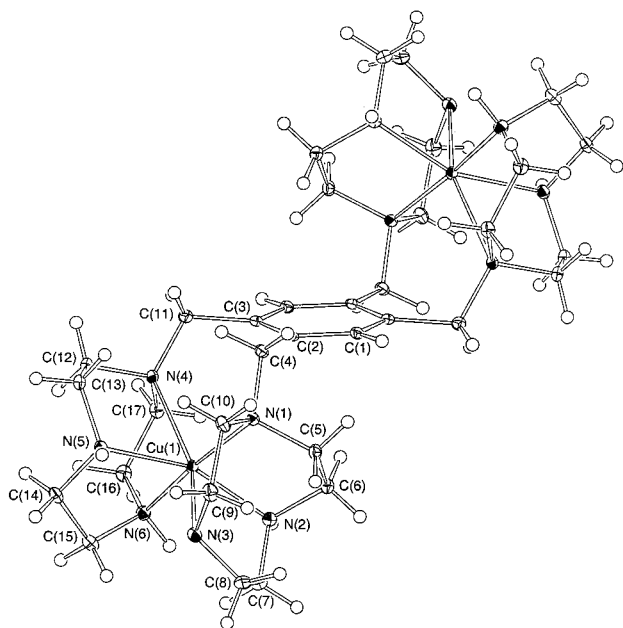


Figure 2. The binuclear cation unit of **5'** with the atomic labeling scheme.

sandwiched by a pair of *ortho*-oriented tacn rings from L^{dur} , in a fashion similar to the single metal centers in $[\text{NiL}^{\text{ox}}](\text{ClO}_4)_2 \cdot \text{H}_2\text{O}$ and $[\text{CuL}^{\text{ox}}](\text{ClO}_4)_2 \cdot 2\text{H}_2\text{O}$.¹⁹ The orientation of the metal-binding compartments relative to the aromatic spacer also parallels that found in these latter complexes, with the benzene ring of the bridge tilted toward one of the sandwiching tacn rings [containing N(21), N(24), and N(27) in **1** and N(1), N(2), and N(3) in **5'**]. The cations are centrosymmetric about the midpoint of the durene spacer, with the two metal centers situated on opposite sides of the plane of the benzene ring, and consequently the M...M separations are long, viz., 9.09 Å for **1** and 8.90 Å for **5'**.

The geometries about the nickel(II) centers in **1** are significantly distorted from octahedral, paralleling that found for the

sandwiched nickel(II) center in $[\text{NiL}^{\text{ox}}](\text{ClO}_4)_2 \cdot \text{H}_2\text{O}$.¹⁹ The intraring $N_{\text{cis}}-\text{Ni}-N_{\text{cis}}$ "bite" angles and the *trans* angles about the nickel(II) centers are all well below the respective values of 90° and 180° expected for an idealized octahedral structure due to the constraints imposed by the three edge-sharing, five-membered chelate rings of the tacn moiety (Table 2). As well as this trigonal distortion imposed by the tacn rings, the interring $N_{\text{cis}}-\text{Ni}-N_{\text{cis}}$ angles involving either one or both of the bridgehead nitrogens [103.1(2)–106.6(3)°] are enlarged relative to those involving pairs of secondary-amine nitrogens [90.3(3)–97.7(3)°], and the bond involving the tertiary bridgehead nitrogen N(11) is elongated relative to all the other Ni–N bonds [2.193(6) vs 2.094(6)–2.151(6) Å]. These effects can be ascribed to the conformational constraints imposed by the aromatic bridging unit, combined with the introduction of less strongly coordinating tertiary amine nitrogens. By comparison, the Ni–N bond lengths in $[\text{Ni}(\text{tacn})_2](\text{NO}_3)\text{Cl} \cdot \text{H}_2\text{O}$ ²⁹ all lie in the 2.09–2.12 Å range, close to the optimum value of 2.08 Å for an octahedral NiN_6 structure, reflecting the more symmetrical coordination environment provided by the unsubstituted tacn macrocycle. There is a *trans* influence evident in **1**, viz., the Ni–N distances for the secondary-amines *trans* to the tertiary bridgehead nitrogens are shorter [2.094(6) and 2.086(7) Å] than those for the pair of *trans* secondary amines [2.149(7) and 2.134(7) Å]. The cation is centrosymmetric, with *quasi*-2/*m* components, through the pair of C(*λ*) atoms of the durene ring and *m* normal to it and the ring plane, broken at the periphery by the ethylene bridge of the tacn.

The corresponding copper(II) complex, **5'**, also exhibits a metal atom environment that is significantly distorted from octahedral. It displays the expected Jahn–Teller distortion imposed by the d^9 copper(II) ion, with two long Cu–N bonds [2.427(2) and 2.506(2) Å] and four short Cu–N bonds [2.031(2)–2.113(2) Å] (Table 2). Comparison of the structure of **5'** and its mononuclear analogue, $[\text{CuL}^{\text{ox}}](\text{ClO}_4)_2 \cdot 2\text{H}_2\text{O}$,¹⁹ with those of related sandwich-type copper(II) compounds reveals that the structure is influenced by supporting ligand

(29) Zompa, L. J.; Margulis, T. N. *Inorg. Chim. Acta* **1978**, 28, L157.

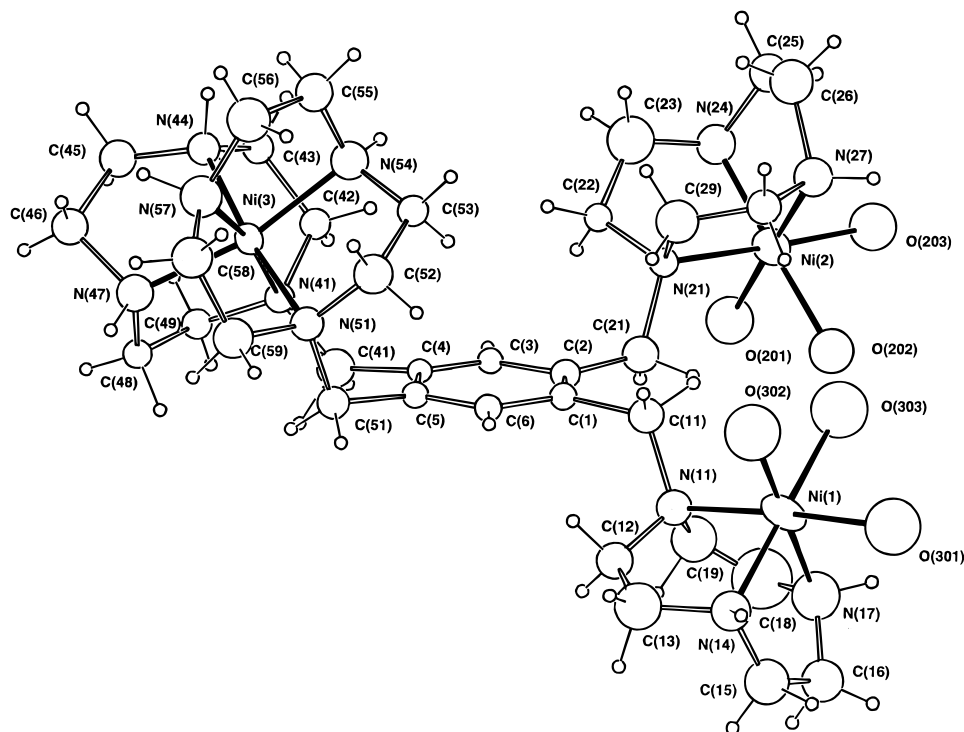


Figure 3. The trinuclear cation unit of **2**, projected through the central benzene ring plane, with the atomic labeling scheme.

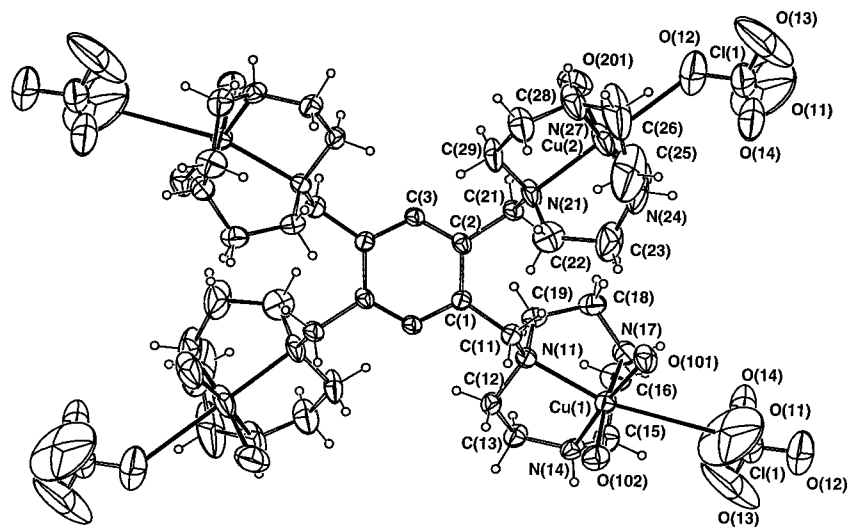


Figure 4. The centrosymmetric tetranuclear cation of unit **4**, projected through the central benzene ring plane, with the atomic labeling scheme.

topology. The crystal structures of $[\text{Cu}(\text{tacn})_2][\text{Cu}(\text{CN})_3] \cdot 2\text{H}_2\text{O}$ ³⁰ and $[\text{CuL}^{\text{prop}}][\text{ZnBr}_4] \cdot \text{H}_2\text{O}$ [$\text{L}^{\text{prop}} = 1,3\text{-bis}(1,4,7\text{-triazacyclonon-1-yl})\text{propane}$],²³ solved at 110 and 293 K, respectively, show tetragonally distorted CuN_6 coordination polyhedra similar to those observed in **1** and $[\text{CuL}^{\text{ox}}](\text{ClO}_4)_2 \cdot 2\text{H}_2\text{O}$ solved at 123 and 173 K, respectively. In $[\text{Cu}(\text{tacn})_2][\text{Cu}(\text{CN})_3] \cdot 2\text{H}_2\text{O}$, however, the Jahn–Teller distortion becomes dynamic above ca. 120 K, so that a subtle effect of tethering the tacn macrocycles in **5'**, $[\text{CuL}^{\text{ox}}](\text{ClO}_4)_2 \cdot 2\text{H}_2\text{O}$, and $[\text{CuL}^{\text{prop}}][\text{ZnBr}_4] \cdot \text{H}_2\text{O}$ is to stabilize a tetragonally elongated structure. In **5'** and $[\text{CuL}^{\text{ox}}](\text{ClO}_4)_2 \cdot 2\text{H}_2\text{O}$, a tertiary bridgehead nitrogen, N(4), and a secondary nitrogen, N(3), occupy the axial sites of the coordination polyhedra, whereas in $[\text{CuL}^{\text{prop}}][\text{ZnBr}_4] \cdot \text{H}_2\text{O}$, the two axial bonds both involve secondary amines, with the bridgehead N(1)

and N(4) atoms occupying equatorial sites of the CuN_6 coordination sphere. Despite this difference in axial coordinating groups, the axial bond lengths are similar in the three complexes {2.427(2) and 2.506(2) Å for **5'**, 2.438(8) and 2.442(8) Å for $[\text{CuL}^{\text{ox}}](\text{ClO}_4)_2 \cdot 2\text{H}_2\text{O}$, 2.402(9) and 2.408(8) Å for $[\text{CuL}^{\text{prop}}][\text{ZnBr}_4] \cdot \text{H}_2\text{O}$ } and are lengthened relative to those found in $[\text{Cu}(\text{tacn})_2][\text{Cu}(\text{CN})_3] \cdot 2\text{H}_2\text{O}$ [2.305(2) and 2.336(2) Å].³⁰ This feature is most likely a result of the constraints imposed by the tethering groups. These constraints do not, however, manifest themselves in the N(1)–Cu–N(4) angles subtending the bridging groups of the complexes {100.05(7)° for **5'**, 99.2(3)° for $[\text{CuL}^{\text{ox}}](\text{ClO}_4)_2 \cdot 2\text{H}_2\text{O}$, 96.8(5)° for $[\text{CuL}^{\text{prop}}][\text{ZnBr}_4] \cdot \text{H}_2\text{O}$ }, since these are similar to the inter-ring $\text{N}_{\text{cis}}\text{—Cu—N}_{\text{cis}}$ angles observed in the nonbridged $[\text{Cu}(\text{tacn})_2][\text{Cu}(\text{CN})_3] \cdot 2\text{H}_2\text{O}$ complex [96.2(1)–101.3(1)°]. By comparison, the N(1)–Cu–N(4) angle in $[\text{CuL}^{\text{eth}}](\text{SO}_4) \cdot 6\text{H}_2\text{O}$ [$\text{L}^{\text{eth}} = 1,2\text{-bis}(1,4,7\text{-triazacyclonon-1-yl})\text{ethane}$]²³ is considerably more acute [76.23(9)°], suggesting that the

(30) Chaudhuri, P.; Oder, K.; Wiegardt, K.; Weiss, J.; Reedijk, J.; Hinrichs, W.; Wood, J.; Ozarowski, A.; Stratemaier, H.; Reinen, D. *Inorg. Chem.* **1986**, *25*, 2951.

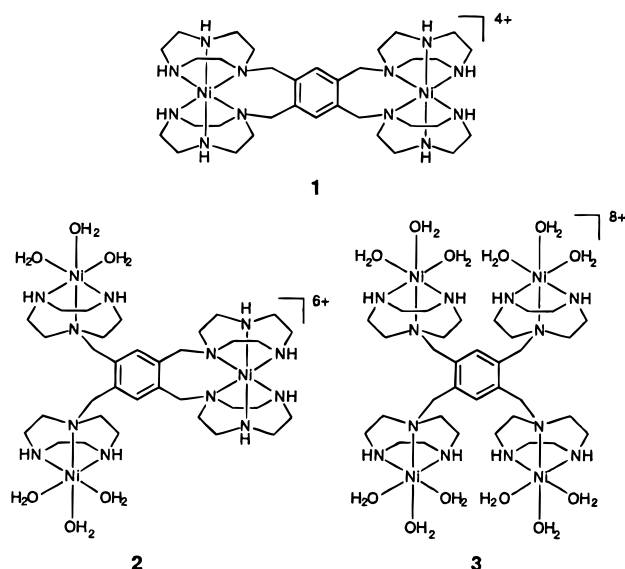


Figure 5. Schematic representations of the “double sandwich” (1), “hybrid” (2), and “full capacity” (3) nickel(II) coordination complexes with L^{dur} .

ethylene tether places a greater strain on the CuN_6 core. Further evidence for this is provided by the fact that the *cis*-disposed $\text{Cu}-\text{N}(1)$ and $\text{Cu}-\text{N}(4)$ bonds are the longest within this latter structure [2.295(2) and 2.347(3) Å]. Despite this, $[\text{Cu}L^{\text{eth}}]^{2+}$ is more stable in solution ($\log K = 27.8$) than $[\text{Cu}L^{\text{prop}}]^{2+}$ ($\log K = 24.9$), possibly a consequence of the more energetically favored five-membered chelate ring supported by the ethylene bridge.²³

The two possible coordination modes of the *ortho*-oriented tacn rings in L^{dur} are exhibited in the crystal structure of **2**, which contains discrete trinuclear $[\text{Ni}_3L^{\text{dur}}(\text{H}_2\text{O})_6]^{6+}$ cations (Figure 3). The X-ray study confirms the hybrid nature of the compound. One nickel(II) center is sandwiched by a pair of *ortho*-oriented tacn rings in a fashion similar to that of the nickel(II) centers in **1**, while the two other centers are each only coordinated by a single tacn ring from the ligand, with their distorted octahedral coordination spheres being completed by ligated water. These mono-tacn-coordinated centers lie on opposite sides of the plane of the benzene ring of the aromatic bridging unit, most likely due to electrostatic and steric effects, with an $\text{Ni}\cdots\text{Ni}$ separation of 6.97 Å. The sandwiched Ni center lies 9.92 and 9.13 Å from Ni(1) and Ni(2), respectively. As was the case for **1**, the intra-ring $\text{N}_{\text{cis}}-\text{Ni}-\text{N}_{\text{cis}}$ bond angles for all three nickel(II) centers are well below the 90° expected for an ideal octahedral geometry (Table 2). The $\text{N}_{\text{trans}}-\text{Ni}-\text{O}_{\text{trans}}$ angles for the mono-tacn-coordinated nickel(II) centers, however, are on average closer to the ideal 180° ($174-179^\circ$) than the $\text{N}_{\text{trans}}-\text{Ni}-\text{N}_{\text{trans}}$ angles observed for the sandwiched nickel(II) centers in both **1** ($170-173^\circ$) and **2** ($167-174^\circ$). This can be attributed to the fact that the NiN_3O_3 coordination spheres are free of the steric constraints introduced by sandwiching a nickel(II) center between two linked tacn macrocycles.

Not surprisingly, the coordination geometry of the sandwiched Ni(3) center in **2** is very similar to that of the nickel(II) centers in **1** and $[\text{Ni}L^{\text{ox}}](\text{ClO}_4)_2 \cdot 2\text{H}_2\text{O}$.¹⁹ Apart from the expected reduction in the intra-ring $\text{N}_{\text{cis}}-\text{Ni}-\text{N}_{\text{cis}}$ “bite” angles and inter-ring $\text{N}_{\text{trans}}-\text{Ni}-\text{N}_{\text{trans}}$ angles, the Ni–N bond lengths (Table 2) show considerably more variation than those found in $[\text{Ni}$

$(\text{tacn})_2](\text{NO}_3)\text{Cl} \cdot \text{H}_2\text{O}$.²⁹ Again the two longest Ni–N bonds are associated with the tertiary bridgehead nitrogens, N(41) and N(51). The distorted octahedral geometries of the Ni(1) and Ni(2) centers are almost identical and parallel those in the binuclear complex, $[\text{Ni}_2L^{\text{px}}(\text{H}_2\text{O})_6](\text{ClO}_4)_4 \cdot 3\text{H}_2\text{O}$, of the *p*-xylylene-bridged bis(tacn) ligand.¹⁹

The molecular structure of compound **4** consists of discrete centrosymmetric tetranuclear $[\text{Cu}_4L^{\text{dur}}(\text{H}_2\text{O})_8]^{4+}$ cations (Figure 4), perchlorate anions, and waters of crystallization (but see below), with quasi-components $2/m$ of the center of symmetry being evident in this array. Both *ortho*- and *para*-oriented sets of metal binding compartments lie *anti* to one another, i.e., on opposite sides of the plane of the benzene ring, consistent with the *anti* conformations observed in the solid state structures of the binuclear metal complexes of the *o*- and *p*-xylylene-bridged bis(tacn) ligands.¹⁹ The *ortho*-oriented copper(II) centers are separated by 7.04 Å, while *para*-oriented copper(II) centers are separated by 9.54 Å. The copper(II) centers reside in distorted square pyramidal (SP) environments with basal planes defined by two water O atoms and two secondary-amine N atoms; the apical position, in each case, is occupied by a tertiary bridgehead N atom. The Cu(1) and Cu(2) centers are displaced 0.12 and 0.10 Å from the least-squares plane of basal atoms in the direction of the apical nitrogen. The Cu–N distances in the basal plane (1.99–2.04 Å) are significantly shorter than the Cu–N(apical) distances of 2.25 and 2.29 Å (Table 2). Long nonbonding contacts are formed with perchlorate O atoms [Cu(1)–O(11) ($2-x, 1-y, 1-z$) 3.28 Å, Cu(2)–O(12) 2.76 Å], pairs of which bridge pairs of cations into centrosymmetric arrays. The degree of trigonal distortion from ideal SP geometry as defined by the geometric parameter $\tau = [(\theta - \phi)/60] \times 100$, where θ and ϕ represent the largest and second largest basal angles, respectively,³¹ gave values [4% for Cu(1) and 0% for Cu(2)] consistent with close to regular SP geometries. These geometric features are typical of copper(II) complexes of ligands incorporating the tacn macrocycle.^{19,22,23}

Conclusion

The coordination properties of a tacn-derived tetramacrocyclic ligand, L^{dur} , have been examined through a study of Ni^{2+} and Cu^{2+} complexation. The ligand is capable of forming bi-, tri-, and tetranuclear complexes, depending on the metal ion and the metal ion-to-ligand ratio employed. For Ni(II), bi- and trinuclear complexes form when a 4:1 metal ion-to-ligand ratio is used and the tetranuclear complex can only be produced by slow addition of L^{dur} to large excesses of Ni^{2+} ions. In contrast, binuclear and tetranuclear copper(II) complexes are readily produced when the appropriate M:L ratio is used. These findings are in keeping with the stereochemical preferences of the two metal centers. Further studies in this area are focusing on the formation of bridged polynuclear complexes facilitated through the introduction of exogenous bridging groups. It is anticipated that these investigations will lead to the further development of magnetostructural correlations in bridging polynuclear metal complexes.

Acknowledgment. Financial support in the form of an Australian Research Council Grant to L.S. and an Australian Postgraduate Award to B.G. is gratefully acknowledged. We thank Dr. G. Lazarev and Ms. S. Duck for the collection of ESR and ESI mass spectral data, respectively.

Supporting Information Available: X-ray crystallographic files, in CIF format, for complexes **1**, **2**, **4**, and **5'**. This material is available free of charge via the Internet at <http://pubs.acs.org>.

(31) Addison, A. W.; Rao, T. N.; Reedijk, J.; van Rijn, J.; Verschoor, G. C. *J. Chem. Soc., Dalton Trans.* **1984**, 1349.